Optoelectronic Sensors
Edited by Didier Decoster & Joseph Harari
Copyright © 2009, ISTE Ltd.

Chapter 4

Phototransistors

4.1. Introduction

The effects of light on transistors have been studied since transistors were first created, with the main motivation for this research being to produce a combination of photodetection and signal amplification in single device. The first work on phototransistors dates from 1951 when Shockley *et al*. [SHO 51] proposed the use of a bipolar n-p-n or p-n-p structure as a phototransistor operating with a base current generated by optical means. The first demonstration of this type of photodetector was achieved two years later when Shive [SHI 53] described a Ge-based n-p-n phototransistor, operating in the spectral region of 1.2 µm wavelength, with an optical gain of the order of 100. In the 1960s, it was mostly bipolar Si phototransistors, operating in the near-infrared, which were developed. However, since the optical absorption coefficient of silicon is weak ($<10^3$ cm^{-1}), the foreseeable applications were not those requiring high speeds.

This interest in phototransistors has recently been revived with the development of optical fiber transmission systems and the evolution of the III-V materials technology. This is because, on the one hand,

---

Chapter written by Carmen GONZALEZ and Antoine MARTY.

the best attenuation and absorption properties of optical fibers are found in the near-infrared, with the three minimal absorption windows at 0.85, 1.3 and 1.55 µm corresponding to the emission and absorption ranges of semiconductor materials based on GaAs and InP. On the other hand, III-V materials have absorption coefficients much higher than that of silicon (>10^4 cm^{-1}). These two characteristics have opened up the possibility of applying phototransistors based on III-V materials to the field of optical telecommunications. Heterojunction bipolar transistors and field effect transistors, made with these materials, began to be studied as phototransistors in the 1970s [ALF 73, BAA 77].

In section 4.2, we present a summary of the different types of phototransistors based on the materials used for their fabrication and as a result their sensitivity to optical wavelengths. We will then classify them according to their structure. In section 4.3 we describe the mechanisms of operation of a bipolar phototransistor and its main properties. Section 4.4 is dedicated to some examples of circuits based around bipolar phototransistors. Finally, in section 4.5, we review the main fields of application of this device.

4.2. *Phototransistors*

In terms of photodetectors, phototransistors can be classed according to their fabrication material and, just like their transistor analogs, they can also be sorted according to structure into two categories: unipolar field effect devices and bipolar devices. This section reflects this dual classification.

4.2.1. *Phototransistors according to their fabrication materials*

The first phototransistors were based on a bipolar homojunction silicon transistor. In this indirect bandgap material, the energy of the bandgap is 1.12 eV. As a result, silicon is photosensitive to wavelengths in the near-infrared, 0.6–0.8 µm. Later, starting in the 1970s, technological progress achieved with III-V compounds and

their ternary and quaternary alloys enabled the development of heterojunction devices: field effect transistors and bipolar transistors. These materials have a direct band structure, and some of their ternary compounds have bandgap energies which match the spectral windows of lowest attenuation in optical fibers: 0.85, 1.3 and 1.55 µm. This is why two variants based on III-V materials have been developed: the GaAs variant (for $\lambda = 0.85$ µm) and more recently the InP variant (for λ = 1.3 and 1.55 µm). Heterojunction phototransistors based on AlGaAs/GaAs are photosensitive to wavelengths between 0.8 and 0.9 µm, with the GaAs bandgap being 1.43 eV. This value of bandgap is compatible with the spectral window of optical fibers around 0.85 µm, for which there is an attenuation of around 2 dB/km. The optical absorption coefficient of GaAs for this wavelength is relatively high: of the order of 10^4 cm^{-1}. The first optical systems, operating initially at 0.85 µm, were later targeted at 1.3 and 1.55 µm where the attenuation in optical fibers is 0.5 and 0.2 dB/km respectively.

Thus, it is the ternary and quaternary alloys based on InP which are best suited for photodetection at these wavelengths. In particular, the ternary alloy $In_xGa_{1-x}As$ with $x = 0.53$, which matches the lattice spacing of InP, has a bandgap energy of 0.75 eV. This value of energy is compatible with photodetection at 1.3 and 1.55 µm. The optical absorption coefficient of InGaAs is 1.16×10^4 cm^{-1} for $\lambda = 1.3$ µm and 6.8×10^3 cm^{-1} for $\lambda = 1.55$ µm. The bandgap energy (E_g) and the applicable spectral range for the main materials used in phototransistor fabrication are shown in Table 4.1.

Material	Si	Ge	GaAs	InP	$In_xGa_{1-x}As$ x = 0.53	$In_xGa_{1-x}As_yP_{1-y}$ x = 0.73 y = 0.60
E_g (eV)	1.12	0.67	1.43	1.34	0.75	0.89
λ (µm)	0.5 – 0.9	0.9 – 1.3	0.75 – 0.85	0.9 – 1.0	1.3 – 1.65	1.0 – 1.2

Table 4.1. *Bandgap energy and applicable spectral range for various materials used in the construction of phototransistors*

4.2.2. *Phototransistors classified by structure*

Homojunction or heterojunction bipolar transistors (photo-HBTs) and unipolar field effect transistors (photo-FETs) are three-terminal devices. When illuminated, the optical input acts as an additional terminal across which the device can be controlled optically. These devices can be integrated into MMICs (*Monolithic Microwave Integrated Circuits*) to achieve optically-controlled amplification or switching, or even more sophisticated microwave functions such as optical locking of oscillators and the mixing of optical and electrical signals [SEE 90].

4.2.2.1. *Unipolar field effect transistors*

Unipolar field effect transistors (FETs), based on III-V materials, only create a single type of charge carrier. Out of the family of field effect transistors, most research has been focused on heterojunction phototransistors which are Schottky gate transistors made with GaAs (MESFETs, *Metal-Semiconductor Field Effect Transistors*) and high electron mobility transistors (HEMT). This popularity is mostly due to the possibilities of using the phototransistor effect in MMICs (Monolithic Microwave Integrated Circuits).

Figure 4.1 shows the cross-section of an illuminated MESFET device (photo-MESFET). Two distinct phenomena occur in the photo-MESFET during illumination by light: a photoconductor effect which is the result of the increase in conductivity due to the creation of photocarriers, and a photovoltaic effect which occurs close to the gate/channel and channel/substrate junctions. Several investigations [GAU 85, MAD 92] have shown not only that the photovoltaic effect dominates the photoresponse of the device, but also that this effect is the cause of the mediocre dynamic performance of photo-MOSFETs. Physically, we can explain this degradation by the poor coupling between the incident light and the gate junction (poor overlap between the optical absorption region and the region with an electric field). A large proportion of the photocarriers end up trapped in low field regions (e.g. the barrier), thus distorting the static characteristics of the device.

Compared to a photo-MESFET without illumination, an important reduction in performance has been observed for the transition frequency f_T and the maximum frequency of oscillation f_{MAX} when illuminated [SIM 86]. The best dynamic performance obtained under illumination is for a bandwidth less than 100 MHz [BAR 97]. Dynamic optical performances are very poor compared to those obtained electrically.

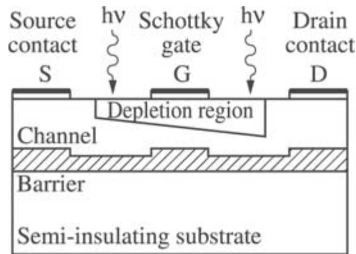

Figure 4.1. *Structure of a GaAs MESFET under illumination. The channel is an n-type semiconducting region sandwiched between a semi-insulating substrate and the space charge region (depletion region) of the reverse-biased Schottky junction*

MESFET-based phototransistors have shown themselves to be a poor approach for developing photodetectors in the microwave and millimeter range. Other devices in the FET family, notably HEMT, suffer from the same limitation [ROM 96]

4.2.2.2. *Bipolar phototransistors*

An alternative to the photo-MOSFET is the silicon-based homojunction bipolar phototransistor or the heterojunction bipolar phototransistor (based on GaAs or InP). In the bipolar phototransistor, there is an overlap between the region of light absorption and the high-electric-field depletion region. This overlap is as good as in PIN photodiodes. As will be shown in section 4.3, the frequency response to a modulated optical signal is directly related to its purely electrical properties. To make the best use of the performance of a transistor, different illumination approaches have been considered, such as

vertical illumination through the front or rear face, lateral illumination, or even the use of a waveguide.

4.2.2.2.1. Traditional surface illumination

The first phototransistors were surface-illuminated, which is the traditional situation, particularly for silicon phototransistors. This vertical illumination allows easy coupling between the optical fiber and the phototransistor, making the integration of the device easier. Several solutions have been proposed: in the case of an opening in the metallic contact of the emitter, the incident light flux crosses the emitter without being absorbed, and the electron-hole pairs are created in the active (or intrinsic) base-collector region of the photo-HBT, that is, the region which is just below the emitter. If a base contact is removed, as shown in Figure 4.2a, the optical flux directly illuminates the base and the collector in the "extrinsic" region of the phototransistor.

4.2.2.2.2. Rear-face illumination

The aim of rear-face illumination of a transistor is the creation of photocarriers in the active region of the transistor (see Figure 4.2b) without modifying the emitter contact. The traditional HBT structure is used with a substrate which does not absorb the incident light. The absorption of light takes place in the collector and the base. Furthermore, the response coefficient is improved because the metallic contact of the emitter acts as a mirror.

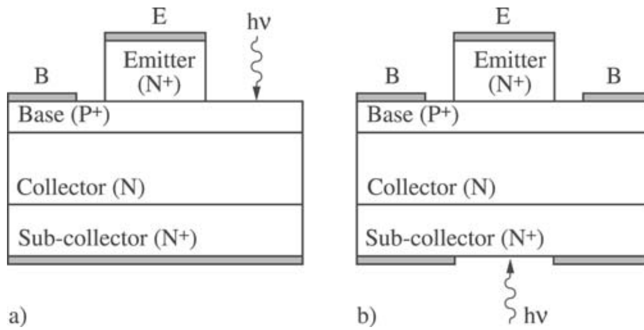

Figure 4.2. *Cross-section of a HBT phototransistor with (a) front-face illumination and (b) rear-face illumination*

4.2.2.2.3. Lateral illumination

Lateral illumination (parallel to the layers) offers another approach for the injection of light into a transistor. It is inspired by the technological processes developed for photodiodes. This type of illumination requires a face very vertical to the base-collector island, in order to obtain the best possible injection efficiency. In laterally-illuminated phototransistors, the photons and charge carries no longer propagate in the same direction, as is the case of vertically illuminated photo-HBTs. The aim of lateral illumination is to simultaneously improve the conversion of optical power into electrical power (quantum efficiency) and the speed performance (high operating frequencies) of the device.

4.2.2.2.4. Lateral illumination with an integrated waveguide

However, lateral illumination does pose significant difficulties in terms of achieving a good optical coupling between the fiber and the device. This is why one trick involves the fabrication of a waveguide integrated into the structure of the device, as shown in Figure 4.3. With this approach, the matching of the mode leaving the optical fiber to the propagation mode inside the device is made easier [FRE 96]. In the best cases, an improvement to the injection efficiency is observed which rises from 50% to 90%, with an improved frequency response.

4.3. The bipolar phototransistor: description and principles of operation

The bipolar phototransistor is a transistor designed such that the "signal" current which feeds the base terminal is mostly provided by photoelectric effects. This "signal" is then amplified by the transistor effect of the device. First we revisit the principle of operation of a bipolar n-p-n phototransistor, which consists of two distinct p-n junctions, as shown in Figure 4.4. Then, we shall discuss the parameters characterizing the phototransistor: the response coefficient, the static and dynamic gains, the response time, the conversion gain and the noise. A cross-section of an n-p-n type bipolar phototransistor, using mesa technology, is shown in Figure 4.4, along with its bias circuit.

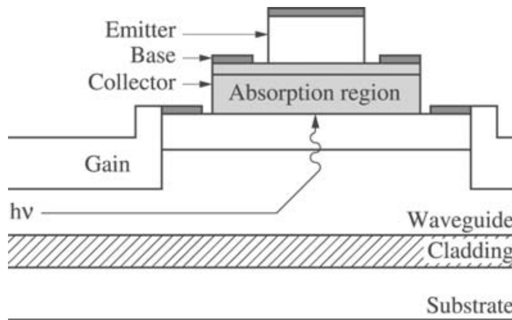

Figure 4.3. *Cross-section of an integrated waveguide phototransistor under illumination*

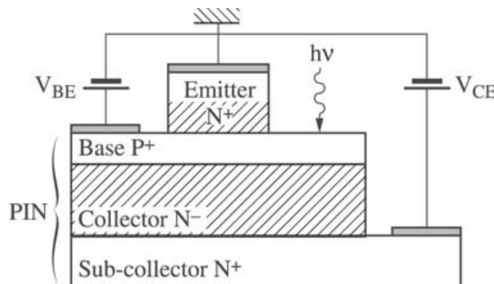

Figure 4.4. *Schematic diagram of an n-p-n phototransistor, along with its bias circuit in common-emitter configuration. The shaded regions are free from mobile charges. The base, collector and sub-collector parts can be thought of as a PIN photodiode*

4.3.1. ***The phototransistor effect***

In Figure 4.4, the n-p-n phototransistor is biased in the common-emitter configuration, with voltages $V_{BE} > 0$ and $V_{CE} > 0$. It differs from traditional bipolar structures, having a relatively large side area of the base-collector junction; this is called the optical window and is what becomes illuminated. This part of the device is effectively a photodiode, connected between the collector and base contacts of the active transistor. When illuminated, electron-hole pairs are created by the photoelectric effect, in the base and in the space charge region (SCR) associated with the base-collector junction (we assume for the sake of simplicity that no absorption takes place in the sub-collector and that the collector is entirely free of mobile charges). A photocurrent I_{Φ}, known as the "primary" photocurrent, is established between the base and collector regions; it is transported by minority electrons from the base which diffuse towards the collector, and by the carriers generated in the SCR, which are separated and moved by the electric field. The flow of this photocurrent I_{Φ} generates a voltage across the base-emitter and base-collector junctions such that the transistor finds itself in its normal operating system ($V_{BE} > 0$ and $V_{CE} > 0$).

The holes attracted by the base will therefore find themselves blocked by the emitter-base junction. This excess of holes will cause a reduction in the emitter-base potential barrier, which results in an injection of electrons from the emitter into the base, from where the majority will diffuse until they are at the level of the collector. Thus, this is the traditional behavior of a bipolar transistor. The amplification of the photocurrent is a purely electrical phenomenon due to the transistor effect.

4.3.1.1. *The main currents in the phototransistor*

In the normal operating system, the phototransistor can be characterized in terms of the following currents (see Figure 4.5):

– Firstly, the emitter injects electrons into the base region. These, minority carriers in this region, diffuse perpendicular to the junction layout and, if the base is thin enough that recombination can be

ignored, they reach the depletion region of the base-collector junction, where the high electric field present in this region clears them out towards the collector region. The flow of these charge carriers gives the contribution I_{ne}, which is shown in Figure 4.5.

– Conversely, a current I_{pe} of holes, majority carriers in the base, is injected from the base towards the emitter.

– Generation-recombination phenomena mostly occur at the level of the emitter-base junction, I_{reb}, and in the base, I_{rb}. I_{reb} comes from the recombination of electrons in the SCR of the emitter-base junction. I_{rb} is caused by the recombination of electrons with holes, majority carriers, in the base.

– Illumination produces the primary photocurrent I_{Φ}. Mostly created in the SCR of the base-collector junction, I_{Φ} originates from a current of electrons which migrate directly toward the collector contact, and from a current of holes which accumulate at the level of the base.

Thus, balancing the different contributions to the current crossing the two junctions, listed above, allows us to calculate the total currents at the emitter, collector and base; in this way, we can use the continuity of the electron and hole currents across the transition regions to write the following equations. For the base:

$$I_E = I_{ne} + I_{pe} + I_{reb} \quad [4.1]$$

the emitter:

$$I_B = I_{pe} + I_{rb} + I_{reb} - I_{\Phi} \quad [4.2]$$

the collector:

$$I_C = I_{ne} - I_{rb} + I_{\Phi} \quad [4.3]$$

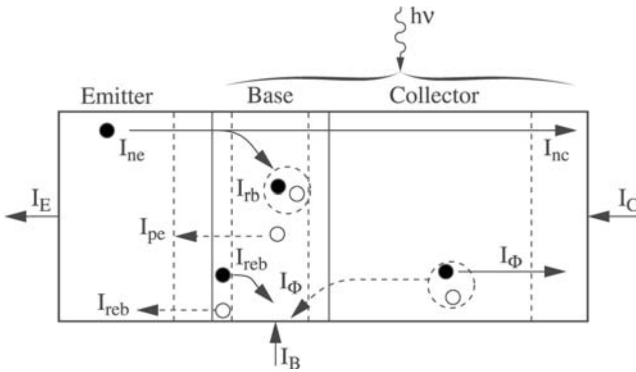

Figure 4.5. *Distribution of the different currents of electrical and optical origin in the phototransistor. The SCRs around the emitter-base and base-collector junctions are shown by dotted lines*

Equations [4.1], [4.2] and [4.3] will be used in the following sections to define the optical gain and the electrical gain of the phototransistor.

4.3.1.2. *Injection efficiency from the emitter in a homojunction and a heterojunction*

The standard parameters for a bipolar transistor, the injection efficiency from the emitter γ, and the transport factor in the base α_T, can be extended to the phototransistor with the help of equations [4.1], [4.2] and [4.3] where the photocurrent term I_Φ was introduced. The injection efficiency γ relates the ratio of the electron current I_{ne} injected into the base to the total emitter current I_E, by the following equation:

$$\gamma = \frac{I_{ne}}{I_{ne} + I_{pe} + I_{reb}} \qquad [4.4]$$

Recombination currents reduce the injection efficiency and they must be minimized. If in equation [4.4] we ignore the effect of recombination in the emitter-base SCR, we obtain:

$$\gamma = \frac{1}{1 + \frac{I_{pe}}{I_{ne}}} \quad [4.5]$$

This ratio must be as close as possible to 1 ($I_{pe} << I_{ne}$) in order to achieve the maximum injection efficiency. Starting from the transport equations established for a bipolar phototransistor, it has been shown that the injection efficiency closely follows the following expression [CAM 85, MOR 72]:

$$\gamma = \frac{A.\gamma_0}{1 + A \cdot \gamma_0} \quad [4.6]$$

where A is a constant, a function of the thickness of the base and the diffusion length of electrons in the base, and γ_0 is the Kroemer factor [KRO 57a and b] established for an emitter-base heterojunction. The Kroemer factor is a function of the physical parameters of the materials making up the heterojunction, and can be expressed in the following way:

$$\gamma_0 = \frac{D_{nb} \cdot L_{pe} \cdot n_e}{D_{pe} \cdot L_{nb} \cdot p_b} \cdot \left(\frac{m^*_{nb} \cdot m^*_{pb}}{m^*_{ne} \cdot m^*_{pe}} \right)^{3/2} \cdot \exp\left(\frac{\Delta E_g}{kT} \right) \quad [4.7]$$

with:

– ΔE_g the difference in bandgap between the emitter and the base;

– D_{nb} the diffusion coefficient of electrons in the base;

– D_{pe} the diffusion coefficient for holes in the emitter;

– L_{pe} the diffusion length for holes in the emitter;

– L_{nb} the diffusion length for electrons in the base;

– n_e the electron density in the emitter;

– p_b the density of holes in the base;

– m^*_{nb} and m^*_{pb} the effective masses of the electrons and holes in the base;

– m^*_{ne} and m^*_{pe} the effective masses of the electrons and holes in the emitter.

For a homojunction bipolar transistor, there is no variation in the bandgap between the emitter and the base, ΔE_g is zero, and the exponential factor in equation [4.7] is equal to 1. It is clear from [4.6] and [4.7] that to obtain a high injection efficiency, $\gamma \approx 1$, it is crucial that the emitter should be much more heavily doped than the base. Conversely, for a heterojunction, γ depends mostly on ΔE_g, and the term $\exp(\Delta E_g/kT)$ becomes dominant compared to the n_e/p_b ratio; thus, to obtain a γ close to 1, it is no longer necessary to under-dope the base relative to the emitter and/or overdope the emitter relative to the base. In heterojunctions based on the materials GaAs/AlGaAs and InGaAs/InP, the size of the emitter bandgap (AlGaAs and InP) is more important than that of the base (GaAs and InGaAs), thus offering a reduction in the injection of majority carriers from the base into the emitter. For the heterojunction phototransistor, the base can be doped at high levels without compromising the efficiency of the junction, leading to a reduction in the resistance of the base. The doping of the emitter can remain within relatively low limits, thus reducing the capacitance of the emitter. These two effects combine to give an improvement in the current gain and an increase in the high frequency performance of the heterojunction bipolar phototransistor.

4.3.1.3. *Transport factor in the base*

The transport factor in the base B is defined by the ratio between the electron current gathered by the collector and the electron current injected from the emitted into the base:

$$B = \frac{I_{nc}}{I_{ne}} = \frac{I_{ne} - I_{rb}}{I_{ne}} \qquad [4.8]$$

Due to the recombination current, B is always less than 1. Beginning with equation [4.8], B can be expressed as a function of the transit time in the base t_B and the lifetime of electrons in the base τ_n using the following equation [CAM 85, CAS 89, POU 94]:

$$B = 1 - \frac{t_B}{\tau_n} \qquad [4.9]$$

According to [4.9], B is closer to 1 when the transit time t_B is small compared to the electron lifetime τ_n. The transit time t_B is smaller when the base thickness is small. As a result, it is necessary for the base thickness to be smaller than the diffusion length of the electrons. For a phototransistor, as for a transistor, the base should therefore be as thin as possible.

4.3.2. *The response coefficient of a phototransistor*

The response coefficient of the photodiode base-collector part of the phototransistor is defined as the ration of the primary photocurrent I_Φ to the received optical power P_{opt}:

$$S_0 = \frac{I_\Phi}{P_{opt}} \left(A/W \right) \qquad [4.10]$$

The quantum efficiency, which is the ratio of the number of electrons collected to the number of incident photons, is also used to characterize the optical-electrical conversion of the base-collector photodiode. This efficiency, often called the external quantum efficiency, is expressed in the following way:

$$\eta = \frac{I_\Phi / q}{P_{opt} / h\nu} = \frac{h\nu}{q} . S_0 \qquad [4.11]$$

and the response coefficient of the phototransistor is characterized by the ratio of the component, due to optical excitation $(I_C)_{opt}$ of the current leaving the device I_C to that same incident optical power:

$$S = \frac{\left(I_C\right)_{opt}}{P_{opt}} = \frac{\left(I_C\right)_{opt}}{I_\Phi} \cdot \frac{I_\Phi}{P_{opt}} \left(A/W \right) \qquad [4.12]$$

As we will see in the following section, the ratio $(I_C)_{opt}/I_\Phi$ defines the optical gain of the phototransistor.

Taking into account equations [4.11] and [4.12] we can express $(I_C)_{opt}$ in the following way:

$$\left(I_C\right)_{opt} = \frac{q}{h\nu}\cdot\eta\cdot G_{opt}\cdot P_{opt} = G_{opt}\cdot S_0\cdot P_{opt} \qquad [4.13]$$

This last equation clearly shows that the phototransistor has an effective response coefficient G_{opt} times greater than that associated with the base-collector photodiode.

4.3.3. *Static electrical and optical gains of the phototransistor*

4.3.3.1. *Static electrical gains β_0 and α_0*

In the static system, the current gain of the phototransistor is obtained without illumination and, as a consequence, it is defined in the same way as for a bipolar transistor. In the common-emitter configuration, the static electrical gain β_0 is given by:

$$\beta_0 = \frac{I_C}{I_B} = \frac{I_{ne} - I_{rb}}{I_{pe} + I_{rb}} \qquad [4.14]$$

This gain can also be expressed as a function of the injection efficiency γ and of the transport factor in the base B taking into account equations [4.5], [4.8] and [4.14]:

$$\beta_0 = \frac{B\cdot\gamma}{1 - B\cdot\gamma} \qquad [4.15]$$

Because of this dependence on γ, the current gain in the common-emitter configuration, β_0, can reach very high values for the heterojunction bipolar transistor. We also define the current gain in common-base configuration α_0, which is the ratio of the collector current to the emitter current. Its relationship with the gain β_0 is:

$$\alpha_0 = \frac{I_C}{I_E} = \frac{\beta_0}{1 + \beta_0} \qquad [4.16]$$

4.3.3.2. *Static optical gain G_{opt}*

The static optical gain of a phototransistor is obtained under continuous illumination. It is defined as the ratio between the component linked to the collector current $(I_C)_{opt}$ and the primary photocurrent I_Φ, obtained at the level of the base-collector photodiode:

$$G_{opt} = \frac{(I_C)_{opt}}{I_\Phi} = \frac{h\nu}{q\eta} \cdot \frac{(I_C)_{opt}}{P_{opt}} \qquad [4.17]$$

G_{opt} is the equivalent of the electrical gain β_0 under illumination. It links the gain obtained through amplification, due to the transistor effect, to the primary photocurrent I_Φ. Several authors have shown that, for a bipolar transistor, G_{opt} is proportional to the product of the external quantum efficiency and the electrical current gain [CAM 85, CHA 85]:

$$G_{opt} \cong \eta \cdot (1 + \beta_0) \qquad [4.18]$$

Equation [4.18] shows that to achieve a given value of G_{opt}, it is necessary to establish a compromise between the quantum efficiency η and the electrical gain β_0, depending on the intended application. The result is that the larger the value of η, the smaller the value of β_0, and vice versa. In addition, G_{opt} is always smaller than β_0.

4.3.4. *Dynamic characteristics of phototransistors*

In the dynamic system, just as for a normal transistor, the phototransistor effect can be put to good use in the quasi-linear "small-signal" mode, in the non-linear mode to achieve multiplication and mixing behavior and in the "large signal" switching system. In these three cases, the illumination varies with time and we are interested either in (amplitude) modulated light or in an impulse. These three dynamic modes of operation of a phototransistor will be analyzed below.

4.3.4.1. *Small-signal operation*

In the context of small-signal applications, the excitation by light may correspond directly to the signal to be amplified, or alternatively it may include a continuous component (modulated signals) which can be put to the particular use of ensuring a pre-bias in addition to that obtained by electrical access to the base. Phototransistors whose base is electrically accessible have the advantage of allowing, by selecting the bias to the base, the choice of an operating point which ensures optimal linearity. The global response time of a phototransistor is no different to the "electrical" response time of the transistor element triggered by the current I_{Φ} induced in the base-collector photodiode. Two time constants are therefore associated with the dynamic operating system of a phototransistor: the first is due to the intrinsic transport of photocurrent carriers, while the second is due to the electrical response of the phototransistor. The first time constant may be more or less important depending on the geometry of the device; however, to begin with, we can presume that it is the electrical response time which is most significant. The electrical response time of a phototransistor is linked to its transition frequency f_{T0}, which is the frequency at which the optical gain is equal to 1. In an equivalent manner to a transistor, this sets the limit for the use of a phototransistor as a photocurrent amplifier. This transition frequency can be calculated in a similar way to the calculation of the equivalent small-signal method for the π hybrid configuration.

4.3.4.1.1. Transition frequency calculated using the π hybrid model

The behavior of a phototransistor in the small-signal system is shown in the equivalent circuit diagram of Figure 4.6b. This is based on an electrical model of a bipolar transistor known as the Giacoletto circuit, which is established for the common-emitter arrangement [LET 78]. The incident illumination is modeled by a photocurrent source i_{Φ} placed between the base B and the collector C. The output signal is taken across the terminals of a load resistance R_L connected to the collector.

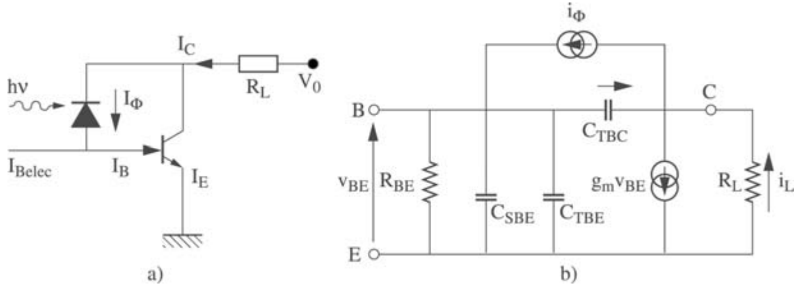

Figure 4.6. *(a) Electrical model and (b) its equivalent electrical circuit in the small-signal system of a phototransistor, for a common-emitter configuration*

The elements of the above equivalent circuit can be described as follows:

– R_{BE} is the dynamic input resistance of the phototransistor;

– $R_{BE} = \beta_0 U_T / I_C$;

– C_{TBE} and C_{TBC} are the transition capacitances of the emitter-base and base-collector junctions;

– C_{SBE} is the diffusion capacitance, which represents the effects of accumulation of minority charge carriers in the base, effects linked to the transit time τ_B in this region, $C_{SBE} = \tau_B . I_C / U_T$;

– g_m defines the transconductance, $g_m = I_C / U_T$.

Under these conditions the input photocurrent i_Φ, called the primary, can be expressed in the following form:

$$i_\Phi = v_{BE} \cdot \left[\frac{1}{R_{BE}} + j\omega \cdot \left(C_{TBE} + C_{SBE} \right) \right] + \left[v_{BE} + R_L \cdot i_C \right] \cdot j\omega \cdot C_{TBC} \qquad [4.19]$$

in which the second term (corresponding to the current component *i* indicated in Figure 4.6) represents the internal reaction mechanism induced by the transition capacitance of the base-collector junction C_{TBC} and by the load resistance R_L, commonly referred to as the Miller effect. If we now ignore the current contributions *i* and i_Φ

compared with the amplified current $g_m v_{BE}$, the output collector current is found to be:

$$i_C \cong g_m \cdot v_{BE} \qquad [4.20]$$

Given this, the ratio i_C/i_Φ, which defines the dynamic current gain of the phototransistor g_{opt}, known as the optical gain in the small-signal system, can be written in the form:

$$\frac{i_C}{i_\Phi}(j\omega) = g_{opt}(j\omega) = \frac{\beta_0}{1 + j \cdot \omega \cdot \beta_0 \cdot \left(\frac{C_{TBE} + C_{TBC}}{g_m} + \tau_B + R_C \cdot C_{TBC} \right)} \qquad [4.21]$$

At high frequencies, the imaginary part of the denominator of equation [4.21] becomes dominant and we can write:

$$g_{opt}(j\omega) \cong \frac{1}{j\omega \left(\frac{C_{TBE} + C_{TBC}}{g_m} + \tau_B + R_L \cdot C_{TBC} \right)} \qquad [4.22]$$

If we assume that the product $R_C.C_{TBC}$ is weak compared to the two first terms, $|g_{opt}|$ is obtained when:

$$\frac{1}{\omega} = \frac{1}{\omega_{TO}} = \frac{C_{TBE} + C_{TBC}}{g_m} + \tau_B \qquad [4.23]$$

Equation [4.23] defines the angular frequency of the transition ω_{T0}, with the transition frequency f_{T0} being $\omega_{T0}/2\pi$. Physically, the transition frequency, f_{T0}, corresponds to the total transit time, τ_T, of photocarriers from the emitter to the collector. It is interesting to analyze this time constant τ_T, associated with f_{T0}. It is defined as:

$$\tau_T = \frac{1}{\omega_{TO}} = \frac{1}{2 \cdot \pi \cdot f_{TO}} \qquad [4.24]$$

If we substitute equation [4.23] into [4.24] we find:

$$\tau_T = \frac{C_{TBE}}{g_m} + \frac{C_{TBC}}{g_m} + \tau_B \qquad [4.25]$$

The first two terms of equation [4.24] correspond to the charging times of the base-emitter and base-collector junctions respectively. Equation [4.25] shows that τ_T depends on the collector current I_C (via g_m) up to a certain threshold and, if we take into account equation [4.13], τ_T is inversely proportional to the incident optical power P_{opt}. For high values of P_{opt}, τ_T approaches the limiting value τ_B. On the other hand, at low values of P_{opt}, the terms in C_{TBE} and C_{TBC} become dominant and the transition frequency f_{T0} is proportional to P_{opt}.

This behavior of f_{T0} as a function of the incident optical power has been experimentally observed, as shown in Figure 4.7. This dependence makes the use of relatively high optical powers (>10 µW) necessary. Alternatively, we can use an electrical current via the metallic base contact to pre-bias the structure, thus reducing the "threshold" optical power needed to reach the maximum value of f_{T0}.

With the help of equation [4.22] we can also define the cutoff angular frequency ω_β as being the angular frequency at which $|g_{opt}|$ falls by 3 dB. This is equal to:

$$\frac{1}{\omega_B} = \beta_0 \left(\frac{C_{TBE} + C_{TBC}}{g_m} + \tau_B + R_L \cdot C_{TBC} \right) \qquad [4.26]$$

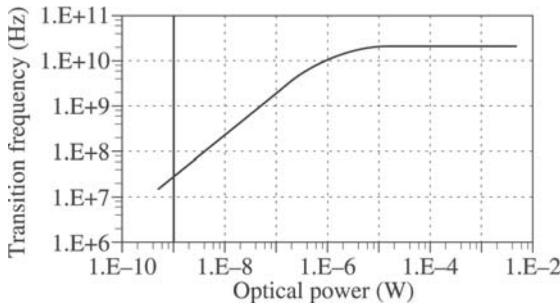

Figure 4.7. *Variation in transition frequency f_{TO} with incident optical power P_{opt}. At weak P_{opt}, f_{TO} varies rapidly up to a certain limiting value of P_{opt}, after which it remains constant*

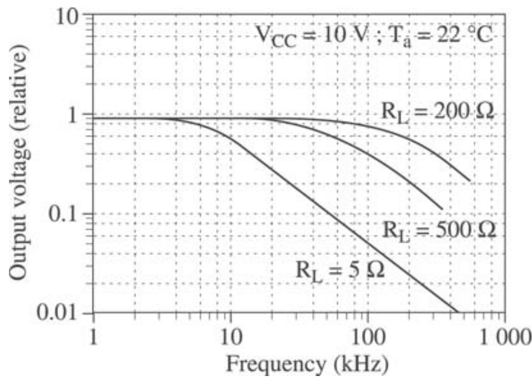

Figure 4.8. *Frequency response of a phototransistor for different load resistances*

It can be clearly seen from equation [4.26] that the cutoff angular frequency ω_β depends on the operating point (as does ω_{TO}) and on the value of the load resistance R_C, as shown in Figure 4.8.

4.3.4.2. *Nonlinear operation*

A bipolar phototransistor behaves similarly to a bipolar transistor, and as a result possesses nonlinear characteristics which allow it to act as an optical-electrical mixer. It can mix a modulated optical signal, carrying information, with an electrical signal from a local oscillator.

This mixing behavior has been the subject of recent research [BET 98, GON 98, SUE 96] and has been developed for telecommunication applications. Two mixing configurations are possible:

– transposition of a low frequency input signal into a higher frequency signal. This mode of operation will be referred to below as up-conversion;

– transposition of a high frequency input signal into a lower frequency signal. This mode will be referred to as down-conversion;

4.3.4.2.1. Mixing principles

Any device able to transpose an input signal from a frequency f_E into another higher or lower frequency is known as a mixer. This change in frequency originates in the nonlinear properties of the mixer and can be explained in the following manner: consider a circuit element whose I/V current-voltage characteristics are nonlinear (a nonlinear resistance, a Schottky diode, etc.). If it is subjected to a voltage $V_{OL} = v_{OL}\sin(\omega_{OL}t)$, its I/V nonlinearity can be described by expanding the current flowing through the element in terms of a discrete series that is a function of the voltage V:

$$I = I(V) = I_0 + a_1 V + a_2 V^2 + a_3 V^3 + \ldots \qquad [4.27]$$

where I_0 is a continuous bias current and a_1, a_2 and a_3 are real constant coefficients. [4.27] shows that we see an infinite number of powers of V appearing at the output of the circuit, these will enrich the spectrum of the input signal V. If we add a second signal to the input, $V_{FI} = v_{FI}\sin(\omega_{FT}t)$, the spectrum of the output signal becomes even more complicated due to the presence of the products of V_{OL} and V_{IF} and their respective harmonics.

If we now replace V with V_{OL} + V_{FI} in [4.27], the current (V) becomes:

$$I = I_0 + a_1\left(V_{OL} + V_{FI}\right) + a_2\left(V_{OL} + V_{FI}\right)^2 + \ldots$$
$$= I_0 + a_1\left(v_{OL}\sin\omega_{OL}t + v_{FI}\sin\omega_{FI}t\right) + a_2\left(v_{OL}\sin\omega_{OL}t + v_{FI}\sin\omega_{FI}t\right)^2 + \ldots$$
$$= I_0 + a_1\left(v_{OL}\sin\omega_{OL}t + v_{FI}\sin\omega_{FI}t\right) \qquad [4.28]$$
$$+ a_2\left\{\frac{1}{2}v_{OL}^2\left(1-\cos 2\omega_{OL}t\right) + v_{OL}v_{FI}\left[\cos\left(\omega_{OL}-\omega_{FI}\right)t - \cos\left(\omega_{OL}+\omega_{FI}\right)t\right]\right.$$
$$\left. + \frac{1}{2}v_{FI}^2\left(1-\cos 2\omega_{FI}t\right)\right\} + \ldots$$

The interesting frequencies are (ω_{OL} + ω_{FI}) and (ω_{OL} – ω_{FI}) and they can be extracted by a filter tuned to the target frequency. In a bipolar mixing transistor, the main nonlinearity contributing to the mixing behavior is transconductance. For a bipolar phototransistor, the nonlinearity in the current gain is the most important parameter.

4.3.4.2.2. Performance criteria

As a first approximation, we can say that the performance criteria established for a mixing transistor can be applied to a mixing phototransistor. We will discuss two of these criteria: conversion gain and insulation.

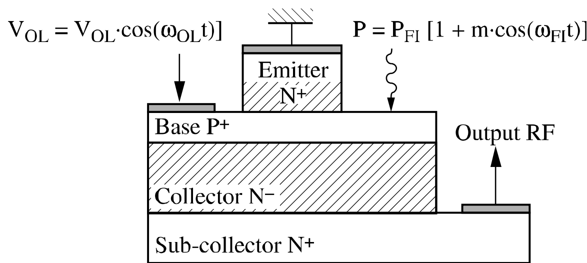

Figure 4.9. *Optical and electric inputs of the phototransistor (in place of the mixing phototransistor)*

Conversion gain

In a mixing phototransistor, the optical input is physically separated from the electrical input (see Figure 4.9). The optical signal “enters” through the optical window and the electrical signal is applied to the metallic contact of the base. In the common-emitter configuration, the mixed signal is obtained at the output of the collector. The traditional definition of the conversion gain G_{con}, applied to a phototransistor, can be expressed as the ratio between the output electrical power at the “mixed” frequency and the effective available input optical power at the modulation frequency of the light. Taking the case of up-conversion, the light is modulated at an intermediate frequency F_{IF}, the frequency of the local oscillator F_{OL} is much higher than F_{IF}, and the mixed frequencies F_{RF} are:

$$F_{RF} = F_{OL} \pm F_{FI}$$

The conversion gain can be written as:

$$G_{con} = \frac{P_{elec}\left(F_{RF}\right)}{P_{opt}\left(F_{FI}\right)} \qquad [4.29]$$

In equation [4.29], the denominator refers to an optical power. In order to determine the electrical power generated by the incident optical power, we must take into account the primary photocurrent I_{Φ} generated by the illumination at the level of the base-collector junction, and of the input impedance associated with this junction, Z_{BC}. The electrical power can thus be expressed by the equation:

$$P_{elec} = \frac{1}{2} \cdot \mathrm{Real}\left(Z_{BC}\right) \cdot \left|I_{\Phi}\right|^2 \qquad [4.30]$$

and the electrical conversion gain can be expressed as:

$$G_{con} = \frac{P_{RF}}{\left(P_{elec}\right)_{FI}} = \frac{2P_{RF}}{\mathrm{Reel}\left(Z_{BC}\right) \cdot \left|I_{\Phi}\right|^2} \qquad [4.31]$$

Another definition of the conversion gain is possible. It is defined as being the ratio between the power of the mixed signal F_{RF} and the "primary" power of the incident signal F_{IF}, in other words, the power of F_{IF} obtained when the base-emitter junction of the phototransistor is short-circuited (base-emitter voltage $V_{BE} = 0$ V).

$$G_{con} = \frac{P_{RF}}{\left(P_{FI}\right)_{V_{BE=0}}} \qquad [4.32]$$

When describing experimental results this second definition of G_{con} is the most widely used.

Insulation

All the frequencies generated by the mixing are present at each of the terminals of the mixer, and this has a significantly detrimental affect on its conversion gain performance. As Figure 4.9 shows, the phototransistor has three points of access, two electrical, the base contact (*OL*) and the collector contact (*RF*), and one optical, the optical window (*IF*). The insulation is measured between two of the mixer's points access, *IF-OL* and *IF-RF*, by the ratio between the power at the frequency F_{OL} (or F_{RF}) present at the access point *OL* (or *RF*) and the power at the frequency F_{OL} (or F_{RF}) present at the IF access point. Let us consider the *OL* and *IF* access points at which the F_{OL} and F_{IF} signals are injected. If we hypothesize that no electrical signal originating from the access point of the base can be converted into an optical signal leaving through the optical window, the *IF-OL* insulation is infinite. The same reasoning can be applied to the *IF-RF* access point. As a result, we obtain a maximum insulation between these two pairs of terminals without needing to use external circuitry. However, for insulations in the opposite direction, *OL-IF* and *RF-IF*, there can be a loss of F_{IF} signal power in each of these two electrical access points.

4.3.4.3. *Operation in the strong-signal system*

As was mentioned previously, the other application of a phototransistor concerns the detection of radiation in the strong-signal system. In this case, the presence or not of the illumination induces a

switching type of behavior: the device initially blocks a signal, or is in the weak conduction system if it is pre-biased. It then enters the normal, or even saturated, system when light is applied; it will then return to the initial mode of operation when the input signal ceases. These system changes give rise to transitory phases, as shown in Figure 4.10, which defines a response time for each: the lag time t_τ is inherent to the time it takes the transistor to start conducting (in the case of operation without pre-bias) and is linked to the charging of the transition capacitances C_{TBE} and C_{TBC}. By considering the mean values of these parameters, this time can be calculated using the expression:

$$t_r = \frac{0.7 \cdot \left(C_{TBE} + C_{TBC}\right)}{I_\Phi} \quad [4.33]$$

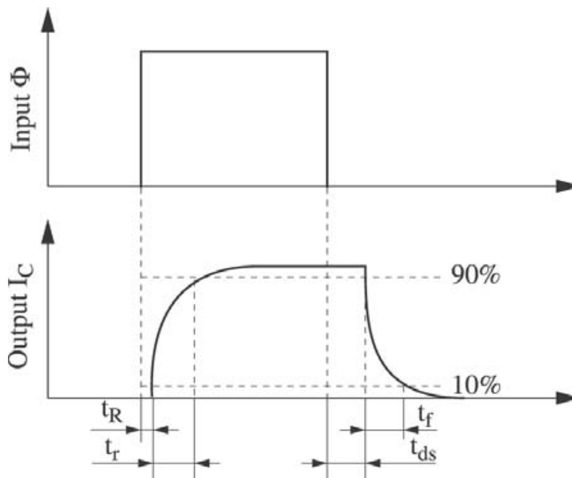

Figure 4.10. *Representation of the different switching response times of phototransistors*

The rise time t_r in the normal active system (up to saturation, if applicable) is more difficult to evaluate, bearing in mind the variation in numerous electrical parameters that apply in this transitory system; nevertheless, the dynamic behavior of the phototransistor can be approached in a simple manner, using the small-signal model. If we assume that the current gain and its cutoff frequency are independent of the level of injection; the result is that the first-order model, which relates I_C to I_Φ in the context of this assumption, suggests that the collector current response to a step change to the primary photocurrent in the base follows an exponential law with time constant $1/\omega_\beta$. Thus, the rise time which separates the start of the growth in the collector current (conventionally, I_C equal to 10% of its final value) from the end of this first transient phase (I_C equal to 90% of its steady-state value), being either $\beta_0.I_\Phi$ or I_{Csat}, can be calculated as:

$$t_m = \frac{2.9}{\omega_\beta} \quad [4.34]$$

when saturation is not reached and:

$$t_m = \frac{0.8}{\omega_T} \cdot \frac{I_{C_{sat}}}{I_\Phi} \quad [4.35]$$

in the alternative case.

For opposite switching, the desaturation time corresponds to the removal of the accumulated surplus charge in the form of the minority carriers (electrons) in the vicinity of the base, and is therefore defined by the lifetime of these charge carriers.

Over the course of the decaying phase of the collector current, the transistor is once more in the normal active system, up to the point it stops conducting. The fall time t_f can again be expressed by equations [4.34] and [4.35].

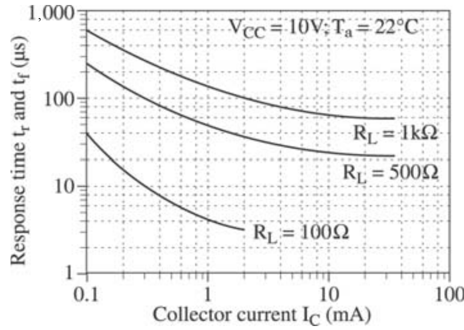

Figure 4.11. *Response time of a phototransistor as a function of the collector current and for different values of the load resistance*

Here once more, in the switching system, the rise time t_r and the fall time t_f increase with the load resistance R_L. We also observe that, while it leads to an increase in response time, the presence of saturation leads to a reduction in these rise and fall times. Finally, the addition of a pre-bias also contributes to an improvement in t_r and t_f, as can be seen in Figure 4.11. Overall, depending on the type of phototransistor and the circuit used, along with its load resistance and operating point, these response times vary from a few tenths to tens of microseconds.

4.3.5. *Noise in phototransistors*

The phototransistor is the first element in a photoreceiver system. This means that there is a certain threshold power below which the photoreceiver cannot detect a signal: a power which is determined by the power of the noise in the phototransistor. The minimum detectable power in the photoreceiver system is limited by the noise in the phototransistor and its load circuit. The noise in the phototransistor is hence an important criterion for judging the performance of the whole photodetection apparatus. The most commonly-used approach for characterizing the noise of a photodetector is the noise equivalent current generator, applied at the input [CAM 82, SMI 80, WAN 86]. This is the approach that we will develop over the rest of this section.

Four main noise sources can be associated with a HPT:

– the shot noise due to the base current I_B entering the phototransistor, this current is the sum of the photocurrent I_Φ and the electrical bias current I_{Belec};

– the shot noise due to the collector current I_C, at the output of the HPT;

– the thermal noise due to the load resistance R_C;

– the thermal noise generated in the base region and, in contrast to the other quasi-neutral regions, the base, although heavily doped, presents an effective base resistance R_B which can reach values as high as hundreds of Ohms.

The spectral densities of the noise power, $\overline{i^2}/\Delta f$ in A^2/Hz, associated with each source of noise are, for the base, the following:

$$\frac{\overline{i_{base}^{2}}}{\Delta f} = \underline{2} \cdot \left(2q \cdot \left(I_\Phi + I_{Belec}\right)\right) + \frac{4kT}{R_{BE}} \qquad [4.36]$$

The factor of $\underline{2}$ in equation [4.36] is due to the correlation which exists between the base-emitter and base-collector junctions [MON 71]. Physically, this arises from the fact that each fluctuation in the base current ΔI_B simultaneously produces another equivalent fluctuation in the emitter current to compensate for ΔI_B. These two currents, in the opposite direction, cancel through recombination, but their shot noises are independent and add up. For the collector:

$$\left.\frac{\overline{i_C^{2}}}{\Delta f}\right|_{output} + \left.\frac{\overline{i_{th}^{2}}}{\Delta f}\right|_{output} = 2qI_C + \frac{4kT}{R_L} \qquad [4.37]$$

These two spectral densities associated with the collector at the output of the transistor are linked to the optical input of the phototransistor in the following manner [THU 99]:

$$\left.\frac{\overline{i_C^{2}}}{\Delta f}\right|_{input} + \left.\frac{\overline{i_{th}^{2}}}{\Delta f}\right|_{input} = \frac{1}{\left|g_{opt}\right|^2} \cdot \left(2qI_C + \frac{4kT}{R_L}\right) \qquad [4.38]$$

where g_{opt} is the dynamic optical gain of the phototransistor, defined in equation [4.21].

Some degree of correlation can exist between the sources of shot noise in the base and collector. Nevertheless, for frequencies above the noise cutoff frequency $1/f$, the correlation between these two sources can be assumed to be negligible [ESC 95]. As a result, the total spectral density of noise power of the phototransistor, in terms of its optical input, can be expressed as the sum of all the spectral densities, equations [4.36] and [4.38]:

$$\frac{\overline{i}^{2}_{Tot}}{\Delta f} = 4 \cdot q \cdot \left(I_{\Phi} + I_{Belec}\right) + \frac{4kT}{R_B} + \frac{1}{\left|g_{opt}\right|^2} \cdot \left(2 \cdot q \cdot I_C + \frac{4kT}{R_L}\right)\left(\frac{A^2}{Hz}\right) \qquad [4.39]$$

According to equation [4.39], the total spectral noise density of the phototransistor is dominated at low frequencies by the sources of noise linked to the photocurrent I_{Φ}, to the bias current of the phase I_{Belec} and to the base resistance R_{BE}; at high frequencies, the noise source due to the collector current becomes dominant.

4.4. Photodetector circuits based on phototransistors

4.4.1. *Amplification circuits*

Phototransistors can be used either in the linear detection system (continuously modulated signals or pulsed signals) or in the switching system, in circuits with (see Figure 4.12a) or without (see Figure 4.12b) pre-bias, with of course the possibility of adding an additional level of amplification (see Figure 4.12c). It has been shown that in every application – detection of weak or strong signals – the speed is limited by the value of the load resistance of the phototransistor. In order to improve sensitivity, it is common nowadays to use either an active load with low input impedance (a common-base transistor) (see Figure 4.12d) or an operational amplifier providing the current-voltage conversion (see Figure 4.12e). Finally, we should note that the phototransistor can be integrated with a second transistor to form a

photo-Darlington pair (see Figure 4.12f). This structure clearly gives a greater response coefficient at the cost of deterioration in the operation speed.

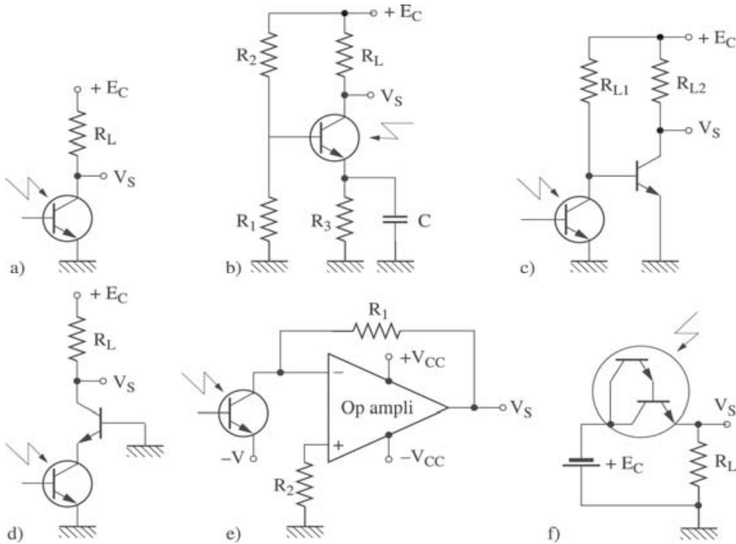

Figure 4.12. *Main circuit diagrams for phototransistors: a) structure with two electrodes E and C, b) pre-bias using access to the base, c) supplementary amplification with a second stage, d) improvement in speed using a low impedance load (common-base transistor) or e) by current-voltage conversion, f) integration on silicon of a second stage: the photo-Darlington pair. Note: structures c) and d) are used in fast circuits*

Structures c) and d) have been used to make monolithic amplification circuits integrating the phototransistor and several HBTs, for wideband [CHA 92, KAM 00, WAN 86a] and narrowband [GON 00a, KAM 95] applications.

4.4.2. *Nonlinear circuits*

Phototransistors can also be used in optoelectric mixing and auto-oscillation configurations. The simplest circuit is shown in Figure

4.13a and consists of a phototransistor and two matching cells. The first cell is placed between the source *OL* and the input to the base of the phototransistor. The second cell is placed between the output of the collector and the load resistance R_L. The optical signal is modulated at the intermediate frequency IF, and the mixed signals at frequencies $OL \pm IF$ are recovered at the output of the collector. The second circuit, described by Sawada *et al*. [SAW 99] and depicted in Figure 4.13b, consists of a phototransistor and a circuit associated with its base which allows it to auto-oscillate at the *OL* frequency of 9.567 GHz. This frequency is stabilized using a dielectric resonator *DR*. The optical signal is modulated at the frequency of 0.2 GHz, and the mixed signals recovered with up-conversion are at frequencies of 9.367 and 9.767 GHz. The third circuit, described by Lasri *et al*. [LAS 00], is shown in Figure 4.13c. It consists of two phototransistors with their emitters joined together. One phototransistor is used as an auto-oscillator at 30 GHz locked optically to an optical signal λ_1 modulated at the same frequency *OL*. This signal *OL* is coupled with the second phototransistor, which acts as an optoelectrical mixer between the 30 GHz signal and a second optical signal, λ_2, modulated at 300 MHz. The two optical signals λ_1 and λ_2 could be at wavelengths corresponding to a WDM (wavelength division multiplexing) scheme. These circuits demonstrate the abilities of phototransistors to combine the functions of photodetection, amplification, mixing and auto-oscillation.

4.5. Applications

4.5.1. *Galvanic isolation*

Silicon phototransistors have been used for a long time in optical isolators. These devices may or may not have a base contact. Figure 4.14 shows an optical isolator based on a phototransistor. For this application, all that is required is to connect a structure upstream which takes care of the conversion of an input electrical signal into a light beam. This is in order to achieve a transfer of information which avoids any form of electrical connection. In this way, galvanic isolation between the controller and the receiver is ensured, and the

achievable voltage difference, which in the static system is determined by the distances which separate the two components or the connections to the different electrodes, can reach several kilovolts.

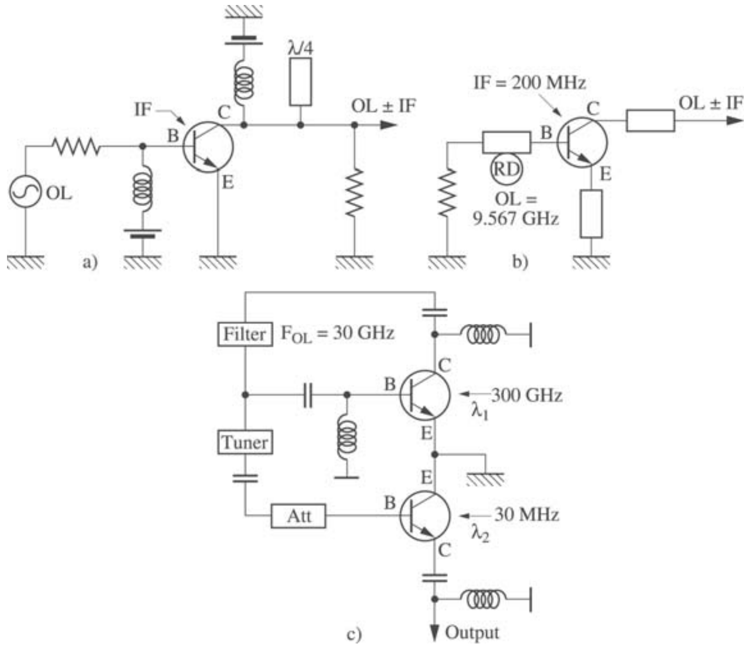

Figure 4.13. *Various circuit diagrams for phototransistors acting as (a) a simple optoelectrical mixer, (b) auto-oscillation and mixing with only one phototransistor and (c) auto-oscillation and mixing with two phototransistors*

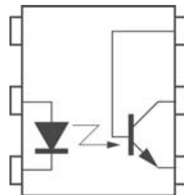

Figure 4.14. *Schematic representation of an optical isolator based on a phototransistor*

The device providing the electron-photon conversion at the input is normally a light-emitting diode (LED) based on GaAs, whose emission line of around 850 nm is well suited to optical detection by the phototransistor or the photo-Darlington pair. The current conversion gain can reach 500%. An example of its variation as a function of the input current is shown in Figure 4.15.

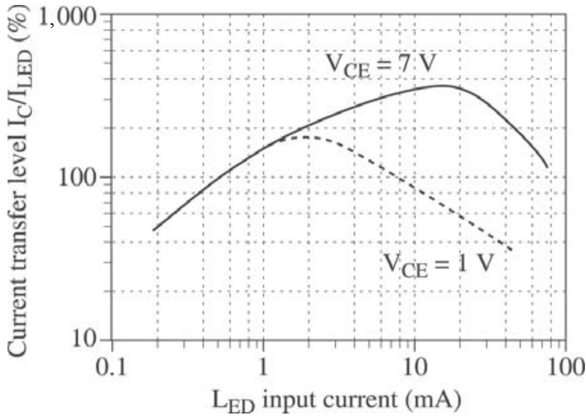

Figure 4.15. *Current transfer level (current from the collector of the phototransistor/current in the input LED) as a function of the input current to the optocoupler*

Another application of silicon phototransistors involves power electronics. These types of devices must often meet strict requirements of galvanic isolation, particularly for control applications and energy conversion from the industrial electricity grid. Control through optical means allows this specific problem to be solved in an efficient and elegant manner: with the thyristor and the triac – which are the two basic bipolar components in this application domain – constructed around a photodiode, whose response replaces the current from the control electrode, the gate. A schematic cross-section for a photothyristor and the equivalent circuit for a phototriac are shown in Figure 4.16.

Photothyristors present very interesting possibilities for direct current power transmission at high voltages (1,000-1,500 A and 5-8 kV) [ARN 92].

The phototriac is constructed by combining two photothyristors in parallel, in opposing directions. The near-obligation, for monolithic integration of this device onto a silicon substrate, of using only one surface of the substrate minimizes the current capacities and reduces the voltage stability. Because of this, these devices are applied in the domain of static relays which involve currents and voltages not exceeding 1 A and 1 kV.

4.5.2. *Phototransistors for optical telecommunications*

This application, which requires both a good response coefficient and speed, mostly involves heterojunction bipolar transistors based on InP and InGaAs.

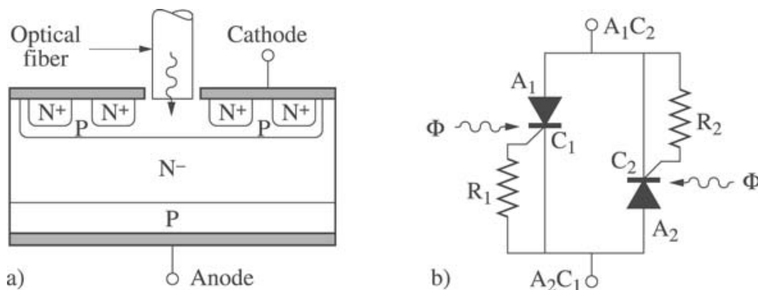

Figure 4.16. *(a) Schematic cross-section of a photothyristor and (b) the equivalent electric circuit for a phototriac*

In the basic process of an optical transmission system, shown in Figure 4.17, the phototransistor is the device which converts the optical signal into an electrical signal. It is situated at the input of the receiver, acting as an optical detector. In the transmitter, the light is modulated (directly or indirectly via an optical modulator) with the signal carrying the information. This signal can be of an analog or

digital. After transport through the optical fiber, the optical signal is demodulated by the photodetector in order to recover the electrical signal. This signal is subject to noise and distortion, and so the receiving circuit may need to amplify and reconstruct the signal in order to extract the original information.

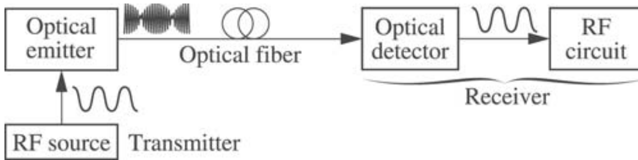

Figure 4.17. *Schematic diagram of an optical transmission system with an analog transported signal*

An InP/InGaAs phototransistor is an alternative to traditional photodetection, consisting of a PIN photodiode associated with a preamplifier. As was previously stated, this device is of interest because of its combination of photodetection and amplification behavior and, since its structure is similar to that of a heterojunction bipolar transistor, it can attain a frequency performance comparable to that of a HBT based on InP [BLA 00]. In addition, when acting as an optical-electrical mixer, it can convert the demodulated signal to other frequency ranges depending on the required output.

4.5.2.1. *InP/InGaAs phototransistors as pre-amplifying photodetectors*

The transport of analog and digital data takes place at frequencies and bitrates that are constantly increasing. In digital transmission, for example, currently 10 and even 50 Gbit/s can be achieved. As a result, phototransistors must become faster and faster while maintaining a good level of sensitivity. The structure of a phototransistor based on InP/InGaAs is shown in Figure 4.18. This device is sensitive to optical wavelengths, λ = 1.3 and 1.55 µm. The base and collector layers are made of InGaAs and the emitter layer is InP. The optical window sits directly above the base. This has been optimized to achieve an optical gain of 30 dB and a transition frequency of 88 GHz [GON 00]. These

high performances are the result of many refinements, particularly to reduce the dimensions of the optical window, the base-emitter and base-collector junctions (in order to reduce their capacitances), as well as the use of a base layer with a graded composition, in order to increase the gain and speed.

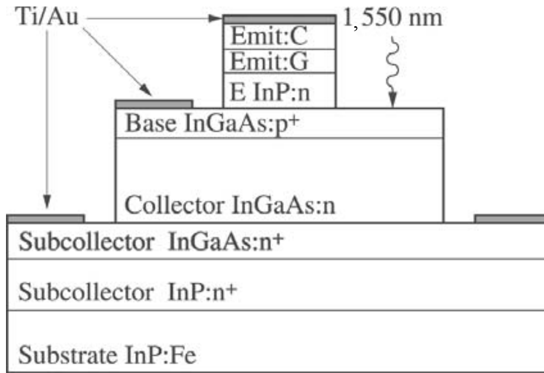

Figure 4.18. *Vertical structure of a phototransistor based on InP/InGaAs on a semi-insulating substrate of InP doped with Fe*

Figure 4.19 shows the response coefficient of the phototransistor in its two modes of operation, transistor (Tr Mode) and photodiode (PIN mode), as a function of the modulation frequency of light. The response coefficient (R) is expressed in dB, R (dB) = 20 log S, with S expressed in A/W. The PIN mode corresponds with the phototransistor operating as a photodiode (V_{BE} = 0V) and the Tr mode operating with the transistor effect (V_{BE} > 0V). As discussed in section 4.3.2, the optical gain G_{opt}, expressed in dB, is equal to the difference between the response coefficient in the Tr mode and that of the PIN mode. The response coefficient in the PIN mode, S_0, is 0.25 A/W. This response coefficient S_0 has been increased to 0.44 A/W in another phototransistor, while maintaining an equivalent optical gain (32 dB). However, as predicted by equation [4.18], the transition frequency drops to 56 GHz [THU 99a].

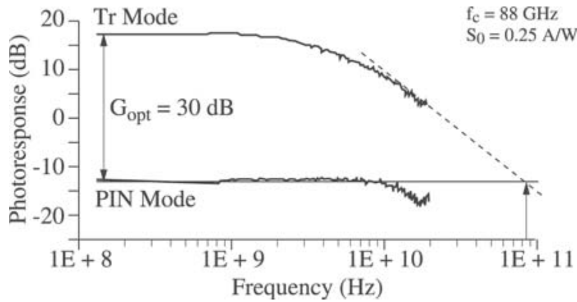

Figure 4.19. *Frequency response of an InP/InGaAs photodiode. The response coefficient (photoresponse) is expressed in dB*

Monolithic photoreceiver circuits for wideband amplification involving photo-HBTs and HBTs have been constructed. The amplifier circuit proposed and built by [KAM 00] exhibits a bandwidth of 40 GHz. The circuit diagram is shown in Figure 4.20. The circuit consists of a phototransistor and two HBT transistors. The two types of device have a double heterojunction and use the same epitaxial layers.

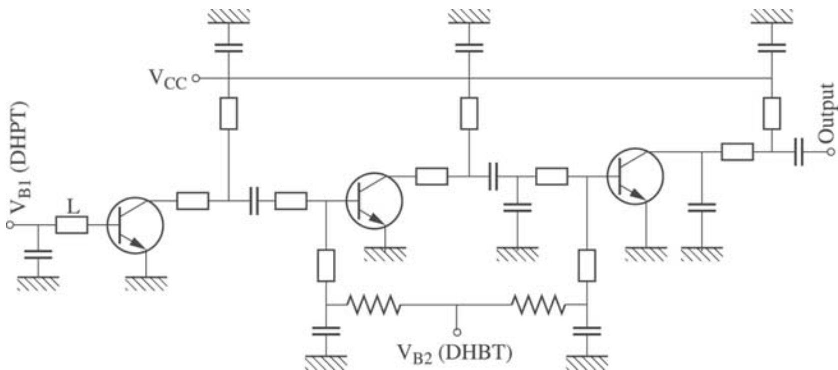

Figure 4.20. *Monolithic circuit diagram for wideband amplification consisting of a phototransistor and two double heterojunction transistors, using InP technology [KAM 00]. The structure of the epitaxial layers is the same for the two devices*

4.5.2.2. *InP/InGaAs phototransistors as an optoelectrical mixer*

The optoelectrical mixing transistor can be used in mixed radio/fiber network access, or in satellite communications, to achieve frequency conversion (up- or down-conversion). It can also be used in high bitrate communication systems as an integral part of timing-signal extraction circuits. Suematsu *et al.* [SUE 96] were among the first to use a photo-HBT based on GaAs, to achieve conversion from the modulation frequency of the light at 2 GHz to a frequency band at 50 GHz. Later, other investigations were reported [GON 98, GON 00], using InP/InGaAs technology, to achieve conversion from an intermediate frequency (≤2 GHz) to frequency bands at 30 and 40 GHz. An example of an experimental setup used to achieve this high frequency conversion is shown in Figure 4.21. The light emitted by a laser source at 1.55 µm is amplitude modulated at an intermediate frequency IF (via an external EOM modulator) in the frequency range of 200 MHz to 2 GHz. The modulated optical signal is injected into the optical window of the phototransistor via a single-mode optical fiber. The base contact is connected to a local oscillator *LO* at a frequency of 30 GHz. After demodulation of the optical signal, the phototransistor mixes the *OL* and *IF* signals and the result is visualized with the help of a spectrum analyzer.

Figure 4.22 shows the output electrical powers of the *IF* signal (in PIN mode) and the mixed signal *OL* + *IF*, as a function of the IF frequency. The conversion gain, using the definition given in [4.32], is the ratio of the output power of the *LO* + *IF* signal to that of the IF signal detected in PIN mode. In the frequency range of IF, from 0.2 to 2 GHz, the conversion gain for the *LO* + *IF* signal is relatively constant, of the order of 7 dB. This positive conversion gain is high because of the direct amplification of the mixed signal by the phototransistor.

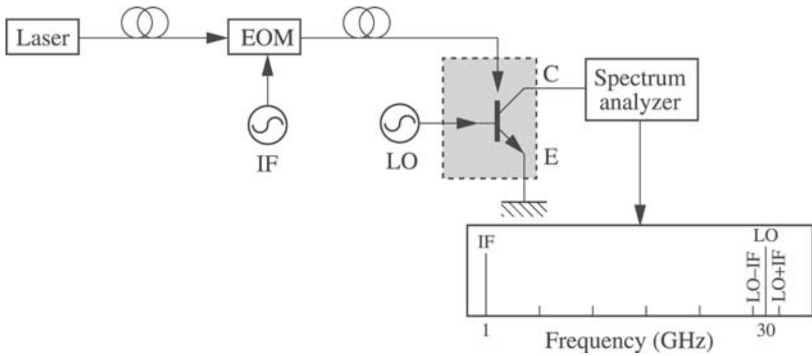

Figure 4.21. *Experimental setup for up-conversion from the intermediate frequency IF to a band at 30 GHz, using the HPT as an O/E mixer*

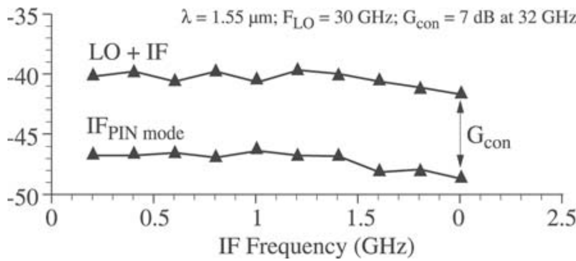

Figure 4.22. *Conversion gain for the IF signal transposed to a frequency of 30 + IF GHz, using the InP/InGaAs phototransistor as an O/E mixer*

4.6. Conclusion

In this chapter we have covered the main characteristics of the bipolar phototransistor. We have also presented its applications in the field of galvanic isolation for silicon phototransistors, and in the field of optical telecommunications for InP/InGaAs heterojunction phototransistors. The study of monolithic circuits incorporating InP/InGaAs phototransistors, and providing more complex functions such as optical-electrical mixing and auto-oscillation, is the particular aim of research intended to exploit the synergy between photonics and

microwaves, with the goal of meeting the ever-growing requirements in sensitivity, speed and functionality of photodetectors.

4.7. Bibliography

[ALF 73] ALFAROV Z.I., AKHMEDOV F., KOROL'KOV V., NIKETIN V., "Phototransistor utilizing a GaAs-AlAs heterojunction", *Sov. Phys. Semicond.*, vol 7, no. 6, p. 780, 1973.

[ARN 92] ARNOULD J., MERLE P., *Dispositifs de l'électronique de puissance*, Hermes, Paris, 1992.

[BAA 77] BAAK C., ELZE G., WALF G., "GaAs MESFET: a high-speed optical detector", *Electron. Lett.,* vol. 13, p. 139, 1977.

[BAR 97] DE BARROS L.E., PAOLELLA A., FRANKEL M., ROMER M., HERCZFELD P., MADJAR A., "Photoreponse of microwave transistors to high-frequency modulated lightwave carrier signal", *IEEE Trans. on Microwave Theory Tech.,* vol. 45, no. 8, p. 1368-1374, 1997.

[BET 98] BETSER Y., RITTER D., LIU C.P., SEEDS A. J., MADJAR A., "A single stage three-terminal heterojunction bipolar transistor optoelectronic mixer", *J. Light. Tech.,* vol. 16, no. 4, p. 605-609, 1998.

[BLA 00] BLAYAC S., RIET M., BENCHIMOL J.L., BERDAGUER P., KAUFFMAN N., GODIN J., SCAVENNEC A., "Lateral design of InP/InGaAs DHBTs for 40 Gbit/s", *Proc. of the Indium Phosphide and Related Materials, IPRM'2000*, p. 481-484, 2000.

[CAM 82] CAMPBELL J.C., OGAWA K., "Heterojunction phototransistors for long-wavelength optical receivers", *J. Appl. Phys*., vol. 53, no. 2, p. 1203-1208, 1982.

[CAM 85] CAMPBELL J.C., "Phototransistors for lightwave communications", *Semiconductors and Semimetals,* vol. 22D, p. 389-447, 1985.

[CAS 89] CASTAGNE R., DUCHEMIN J.P., GLOANEC M., RUMELHARD C., *Circuits intégrés en arséniure de gallium*, Masson, 1989.

[CHA 85] CHAND N., HOUSTON P.A., ROBSON P.N., "Gain of a heterojunction bipolar phototransistor", *IEEE Transactions on Electron Devices*, vol. ED-32, no. 3, p. 622-627, 1985.

[CHA 92] CHANDRASEKHAR S., LUNARDI L.M., GNAUCK A.H., RITTER D., HAMM R.A., PANISH G.L., QUA G.L., "A 10 Gbit/s OEIC photoreceiver using InP/InGaAs heterojunction bipolar transistors", *Electronics Letters,* vol. 28, no. 5, p. 466-468, 1992.

[ESC 95] ESCOTTE L., ROUX J. P., PLANA R., GRAFFEUIL J., GRUHLE A., “Noise modelling of microwave heterojunction bipolar transistors”, *IEEE Transactions on Electron Devices*, vol. 42, no. 5, p. 883-888, 1995.

[FRE 96] FREEMAN P., ZHANG X., VURGAFTMAN I., SINGH J., BHATTACHARYA P., “Optical control of 14 GHz MMIC oscillators based on InAlAs: InGaAs HBTs with monolithically integrated optical wave guides”, *IEEE Transactions Electrons Devices*, vol. 43, no. 3, p. 373-379, 1996.

[GAU 85] GAUTIER J.L., PASQUET D., POUVIL P., “Optical effects on the static and dynamic characteristics of a GaAs MESFET”, *IEEE Trans. on Microwave Theory Tech.,* vol. 33, no. 9, p. 819-822, 1985.

[GON 98] GONZALEZ C., THURET J., RIET M., BENCHIMOL J.L., “Optoelectronic up-converter to millimetre-wave band using an heterojunction bipolar phototransistor”, *Proc. of the European Conference on Optical Communication, ECOC’98*, vol. 1, p. 443-444, 1998.

[GON 00] GONZALEZ C., MULLER M., BENCHIMOL J.L., RIET M., JAFFRÉ P., LEGAUD P., “HBT phototransistor for remote upconversion in hybrid fibre radio distribution systems”, *Proc. of the European Conference on Optical Communication, ECOC 2000*, vol. 2, p. 103-104, 2000.

[GON 00a] GONZALEZ C., MULLER M., BENCHIMOL J.L., RIET M., JAFFRÉ P., LEGAUD P., “A 28 GHz HPT/HBT monolithically integrated photoreceiver for hybrid fibre radio distribution systems”*, Proc. of the 8th IEEE International Symposium on Electron Devices for Microwave and Optoelectronic Applications, EDMO 2000*, p. 55-60, 2000.

[KAM 95] KAMITSUNA H., “Ultra-widebande monolithic photoreceivers using HBT compatible HPTs with novel base circuits and simultaneously integrated with an HBT amplifier”, *J. Lightwave Tech.,* vol 13, no. 12, p. 2301-2307, 1995.

[KAM 00] KAMITSUNA H., MATSUOKA Y., YAMAHATA S. AND SHIGEKAWA N., “A 82 GHz-Optical-gain-cutoff-frequency InP/InGaAs double-hetero-structure phototransistor (DHPT) and its application to a 40 GHz band OEMMIC photoreceiver”, *Proc. of the European Microwave week 2000*, *EuMC 2000*, *EuMC36*, 2000.

[KRO 57a] KROEMER H., “Quasi-electric and quasi-magnetic fields in non-uniform semiconductors”, *RCA Rev.* vol. 18, p. 332, 1957.

[KRO 57b] KROEMER H., “Theory of a wide-gap-emitter for transistors”, *Proc. IRE*, vol. 45, p. 1535, 1957.

[LAS 00] LASRI J., BILENCA A., EISENSTEIN G., RITTER D., ORENSTEIN M., SIDEROV V., GOLDGEIER S., COHEN S., “A two heterojunction bipolar photo-transistor configuration for millimeter wave generation and modulation”, *Proc. of the International Topical Meeting on Microwave Photonics, MWP’00*, p. 62-65, 2000.

[LET 78] LETURCQ P., REY G., *Physique des composants actifs à semiconducteurs*, Dunod University, 1978.

[MAD 92] MADJAR A., PAOLELLA A., HERCZFELD P.R. "Analytical model for optically generated currents in GaAs MESFET", *IEEE Trans. on Microwave Theory Tech.,* vol. 40, p. 1681-1691, 1992.

[MON 71] de LA MONEDA F.H., CHENETTE E.R., VAN DER ZIEL A., "Noise in phototransistors", *IEEE Transactions on Electron Devices,* vol. ED-18, no. 6, p. 340-346, 1971.

[MOR 72] MORIIZUMI T., TAKAHASHI K., "Theoretical analysis of heterojunction phototransistors", *IEEE Transactions on Electron Devices,* vol. 19, no. 2, p. 152-159, 1972.

[POU 94] POUVIL P., *Composants semiconducteurs micro-ondes*, Masson, 1994.

[ROM 96] ROMERO M., MARTINEZ M., HERCZFELD, "An analytical model for the photodetection mechanisms in high-electron mobility transistors", *IEEE Trans. on Microwave Theory Tech.,* vol. 44, no. 12, p. 2279-2287, 1996.

[SAW 99] SAWADA H., IMAI N., "An experimental study on a self-oscillating optoelectronic up-converter that uses a heterojunction bipolar transistor", *IEEE Trans. on Microwave Theory Tech.*, vol. 47, no. 8, p.1515-1521, 1999.

[SEE 90] SEEDS A. J., DE SALLES A.A.A., "Optical control of microwave devices", *IEEE Trans. on Microwave Theory Tech.*, vol. 38, no. 5, p. 577-585, 1990.

[SHI 53] SHIVE J.N., "The properties of germanium phototransistors", *J. Opt. Soc. Am.*, vol. 43, p. 239, 1953.

[SHO 51] SHOOCKLEY W., SPARKS M., TEAL G.K., "p-n junctions transistors", *Phys. Rev*., vol. 83, p. 151, 1951.

[SIM 86] SIMONS R., BHASIN K., "Analysis of optically controlled microwave/millimeter- wave device structures", *IEEE Trans. on Microwave Theory Tech.,* vol. MTT-34, no. 12, p. 1349-1355, 1986.

[SMI 80] SMITH R.D., PERSONICK S.D., *Semiconductor Devices for Optical Communications*, Springer, Berlin, Heidelberg, p. 89, 1980.

[SUE 96] SUEMATSU E., IMAI N., "A fiber optic: millimeter-wave radio transmission link using HBT as direct photodetector and an optoelectronic upconverter", *IEEE Trans. on Microwave Theory Tech.,*vol. 44, no. 1, p. 133-142, 1996.

[THU 99] THURET J., Phototransistor bipolaire à hétérojonction InP/InGaAs pour conversion optique/bande millimétrique dans les réseaux de distribution hybride radio sur fibre, Thesis, University of Paris VI, 1999.

[THU 99a] THURET J., GONZALEZ C., BENCHIMOL J.L., RIET M., BERDAGUER P., "High-speed InP/InGaAs heterojunction phototransistor for millimetre-wave fibre radio communications", *Proc. of the Indium Phosphide and Related Materials, IPRM'99*, p. 389-392.

[WAN 86] WANG H., Photorécepteur monolithique intégrant un phototransistor et des transistors bipolaires à heterojonction GaAlAs/GaAs pour transmission par fibre optique, Thesis, University of Paris XI, 1986.

[WAN 86a] WANG H., ANKRI D., "Monolithic integrated photoreceiver implemented with GaAs/GaAlAs heterojunction bipolar phototransistor and transistors", *Electronics Letters,* vol. 22, no. 7, p. 391-393, 1986.